

# A polypropylene/high density polyethylene blend compatibilized with an ethylene-propylene-diene monomer block copolymer: Fitting dynamic rheological data by emulsion models with a physical scheme

Hua-Yong Liao, Guo-Liang Tao, Chun-Lin Liu, Fang-Hong Gong

School of Materials Science and Engineering, Changzhou University, Changzhou 213164, China

Correspondence to: H.-Y. Liao (E-mail: roynetlhy@163.com)

**ABSTRACT:** The dynamic rheological behaviors at 210, 230, and 250 °C are measured by small amplitude oscillatory shear on a rotational rheometer for a polypropylene(PP)/ ethylene-propylene-diene monomer(EPDM) block copolymer/ high density polyethylene (HDPE)/blend. The scanning electron microscope (SEM) photomicrographs show the blend has a droplet/matrix, semi-co-continuous, co-continuous morphology respectively at different weight ratios. The Cole–Cole ( $G''$  vs.  $G'$ ) data of the blends can be fitted by the simplified Palierne's model only for very narrow weight ratios. A physical scheme is proposed that the dispersed droplets are enclosed by EPDM, thus an equivalent dispersed phase is made up of “expanded” EPDM. With this physical scheme the  $G''$  vs.  $G'$  data of the HDPE-rich blends at 210 °C can be fitted well by Palierne's model. Also with the physical scheme the  $G''$  vs.  $G'$  data of the PP-rich blends at three temperatures can be fitted well by G–M's model with  $G^*$  of interface equals to zero. This means the proposed physical scheme is reasonable. © 2016 Wiley Periodicals, Inc. *J. Appl. Polym. Sci.* **2016**, *133*, 43709.

**KEYWORDS:** blends; rheology; theory and modeling; viscosity and viscoelasticity

Received 4 September 2015; accepted 28 March 2016

DOI: 10.1002/app.43709

## INTRODUCTION

Polymer blending has been a common and economic method to develop new polymer materials for many years. But for most polymer blends the components are thermodynamically immiscible due to of the complexity of polymers. Molecular weight, molecular weight distribution, molecular structure and etc. affect the miscibility of polymer blends. The interfacial adhesion between components of immiscible blend is often insufficient, which results in poor mechanical properties. In order to increase the miscibility of polymer blends physical or chemical compatibilizer is usually added into the blends. Plenty of works have been focused on the compatibility of polymer blends.

Rheology especially dynamic rheology is sensitive to the phase behavior and structure of polymer blends.<sup>1–4</sup> In investigating the linear viscoelasticity of polymer blends, some models play an important role. The models such as Palierne's emulsion model,<sup>5,6</sup> Bousmina's model,<sup>7,8</sup> Lee and Park's model,<sup>9,10</sup> Gramespacher and Meissner's model (simply named G–M's model),<sup>11</sup> *et al.* are often used to predict the linear viscoelasticity of polymer blends. Palierne's model<sup>12,13</sup> has been applied to fit the dynamic rheological data of two LDPE/HDPE binary blending melts and blends of a long-chain branched polypropylene and different polypropylenes respectively. From a new viewpoint the G–M's

model consisted of two parts of pure components and the interface. Although G–M's model is an empirical model derived from the model of Choi and Schowalter (simply named C–S's model),<sup>14</sup> it provides physical insights on interfacial relaxation contrary to the Palierne's model due to the separability of formula.<sup>15</sup> In their work,<sup>15</sup> the authors investigated the Palierne's model through the picture of Gramespacher–Meissner's model and obtained the weighted relaxation time spectra.

The phase structure of polymer blend is complex and affected by various factors. Under a certain condition and at different compositions the polymer blends may show different morphologies, such as droplet/matrix, co-continuous morphology, phase inversion, emulsion-in-emulsion morphology<sup>16</sup> and *et al.* Although the models succeed in predicting dynamic rheological behavior, they still have some limitations. For examples, Palierne's model<sup>5</sup> is suitable for droplet/matrix morphology with some assumptions, and the concentration of the inclusion is generally less than 15 vol %. For a PLA/PCL blend with large difference of zero-shear viscosity between the components, G–M's model fails to fit the data and predict proper interfacial tension.<sup>17</sup> Palierne's model and the C–S's model assume there are no interactions between the dispersed droplets. Neglecting the particle–particle interactions may lead to failure of prediction in using emulsion model. Lee and Park's model considers the steric interactions

and anisotropic effects in concentrated systems. For polymer blends with co-continuous morphology, most emulsion models fail to predict dynamic modulus. Droplet-droplet coalescence leads to formation of co-continuity. Based on a mechanical model Yu<sup>18</sup> and co-workers proposed a rheological model to predict the dynamic rheological data with co-continuous morphology. Due to the difficulty and complexity of co-continuous morphology, more emulsion models are seldom proposed in literatures as far as the authors know. More experimental and theoretical work need to be done to probe the linear viscoelasticity of polymer blends.

Since polymer blends may present complex morphology such as emulsion-in-emulsion,<sup>16</sup> direct application of Palierne's model may lead to poor fitting result. In that system, some PP or PP-g-MAH was enclosed by PA6 particles which were dispersed in the PP matrix. Thus it is necessary to consider "effective" dispersed phase and matrix. Regarding the PP-in-PA6 particles as pure PA6 particles, then the "effective" volume fraction of the PA6 phase increased, and fitting result by Palierne's model was rather well. A similar phenomenon happens in our work for a PP/EPDM/HDPE blend with fixed weight fraction 3% of EPDM. For the HDPE-rich blend taking PP/EPDM as dispersed phase, and for the PP-rich blend taking HDPE/EPDM both produce unsatisfying fitting curve by Palierne's model. Since the complex viscosity and dynamic modulus of the blends are much higher than that of pure HDPE or PP and lower than that of EPDM, it infers the role of pure EPDM is the key factor. Then a physical scheme is proposed, i.e., the "effective" dispersed phase is considered to be EPDM which including the minor phase. With this physical scheme most of the dynamic rheological data are well fitted using Palierne's model as well as G-M's model. A new approach to deal with dynamic rheological fitting for ternary blends is introduced in this work.

## EXPERIMENTAL

### Materials

HDPE 5306j, produced by Yangzi, China. Its melt flow rate (MFR) is 12.8 g·(10 min)<sup>-1</sup>, measured at 210 °C, 2.16 kg. PP T30S, produced by Dalian, China. Its melt flow rate (MFR) is 6.1 g·(10 min)<sup>-1</sup>, measured at 210 °C, 2.16 kg. EPDM 3720P, produced by Dow Chemical Company. Its PE content is 69 wt %, PP content is 30.5 wt %. Mooney viscosity of EPDM is 20 MU measured at ML 1 + 4, 125 °C.

### Preparation of Blends

The materials were dried at 80 °C for 12 h in an electric blast drying oven, then were mixed in a high-speed mixer (produced by Fuxin Light Industry Machinery Factory, Liaoning, China) with the weight ratio PP/EPDM/HDPE of 0/3/100, 10/3/90, 30/3/70, 50/3/50, 70/3/30, 90/3/10, and 100/3/0. After that the samples were fed into a co-rotating twin screw extruder (type SHJ-35, made in Rubber and plastic machinery factory in Guangzhou, China), melt and extruded through a die, then were cooled under water, granulated by a granulator, and were dried at 120 °C for 12 h in an electric blast drying oven. The rotating speed of the screw extruder was 110 r/min, the feeding speed was 100 r/min, and the temperature of the nine zones of

the barrel was 150, 170, 190, 200, 210, 210, 210, and 210 °C, the temperature of the die was 210 °C.

### Measurement

Scanning electron microscope (SEM): the sample was fractured in an Izod impact test machine ADN-5.5 produced by Hengshang industrial equipment, Suzhou, China. The cross section was sprayed with gold and was observed by SEM LE0438VP made by Hitachi Company, Japan. The average dispersed phase size is calculated by a software Nano Measurer 1.2.0.

Rheological measurement: small amplitude oscillatory shear was applied by using a rotational rheometer MCR301 made by Anton Paar GmbH of Germany with two parallel plates. The diameter of the plate is 25 mm, the gap of the two plates was 1 mm. The temperature in the experiment was 210, 230, and 250 °C, and the angular frequency was from 0.028 to 300 rad s<sup>-1</sup> in an ascending order. Below 210 °C, the viscosity of the blends will increase and the rheological measurements will become difficult. Above 250 °C the rheological cell becomes very hot and it is not easy to cool it down quickly although ice bags are used in the circulating water. Below 0.01 rad s<sup>-1</sup> the experimental time becomes very long. The measurement was under nitrogen gas to avoid oxidization of the samples. Before the start of the measurement the samples were kept for 5 min between the gap of the two plates to eliminate thermal history. The linear viscoelastic regime was determined by applying strain sweeping.

## RESULTS AND DISCUSSION

### Dynamic Rheological Curves of PP/EPDM/HDPE Blending Melts

Figure 1(a) shows the droplet-matrix morphology of PP/EPDM/HDPE = 10/3/90 blend, PP is the dispersed phase and HDPE is the matrix. The average droplet diameter of 10/3/90 blend is 0.48 μm. Figure 1(b) shows the morphology of PP/EPDM/HDPE = 30/3/70 blend, which is a semi-co-continuous morphology, although some elongated droplets can be observed. Figure 1(c) shows a continuous morphology of 50/3/50 blend. Figure 1(d) shows a droplet/matrix morphology of 70/3/30 blend, the minor phase HDPE is the dispersed phase, the matrix is PP. The average droplet diameter of 70/3/30 is 0.54 μm, similar to that of the 10/3/90 blend. The droplet size is affected by a dynamic equilibrium between breakup and coalescence process. For the PP-rich blends, the dispersed phase HDPE can deform much easier than the dispersed phase PP in HDPE-rich blends.

Figures 2–4 show the complex viscosity and dynamic modulus of pure HDPE, PP and EPDM at three temperatures 210, 230, and 250 °C, respectively. As temperature increases the complex viscosity and dynamic modulus decreases. At the same temperature, EPDM has higher viscoelasticity than PP, and PP has higher viscoelasticity than HDPE. For example at the angular frequency of 0.028 rad s<sup>-1</sup>, EPDM, PP, and HDPE has a viscosity of 24100, 5660, and 1670 Pa s, respectively at 210 °C.

Figure 5 shows the dynamic rheological curves of the PP/EPDM/HDPE blends at 210 °C. The blends at 230 and 250 °C have similar rheological behaviors, thus the dynamic rheological curves are not shown here. Within the applied frequency range, the shear viscosities of the blends at 210 °C show shear thinning

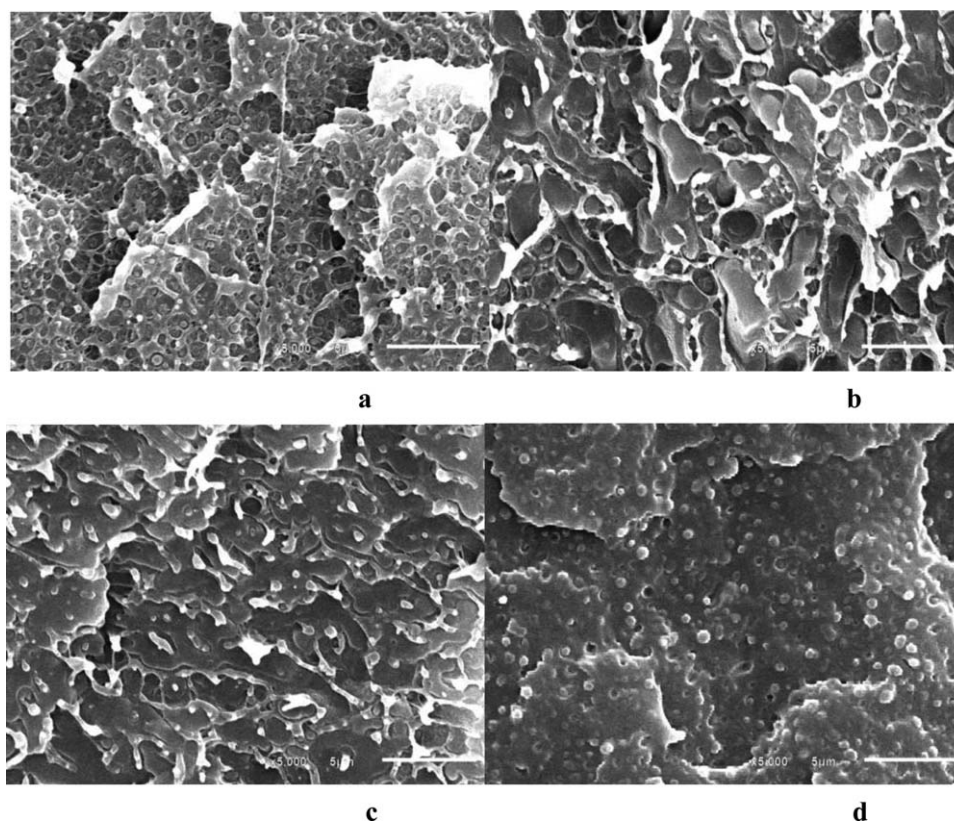


**Figure 1.** SEM photo of (a) PP/EPDM/HDPE = 10/3/90 ( $\times 5000$ ), (b) PP/EPDM/HDPE = 30/3/70 ( $\times 5000$ ), (c) PP/EPDM/HDPE = 50/3/50 ( $\times 5000$ ) (d) PP/EPDM/HDPE = 70/3/30 ( $\times 5000$ ) blends.

behavior. As the increase of PP from 0 to 90 weight fraction, the viscosity at low frequency increases. As for the storage modulus ( $G'$ ), the  $G'$  at low frequency of the four blends 30/3/70, 50/

3/50, 70/3/30 and 90/3/10 lay beyond the  $G'$  range between 0/3/100 and 100/3/0 blends. This is the case for the blends at three temperatures. And the 70/3/30 blend shows highest value of

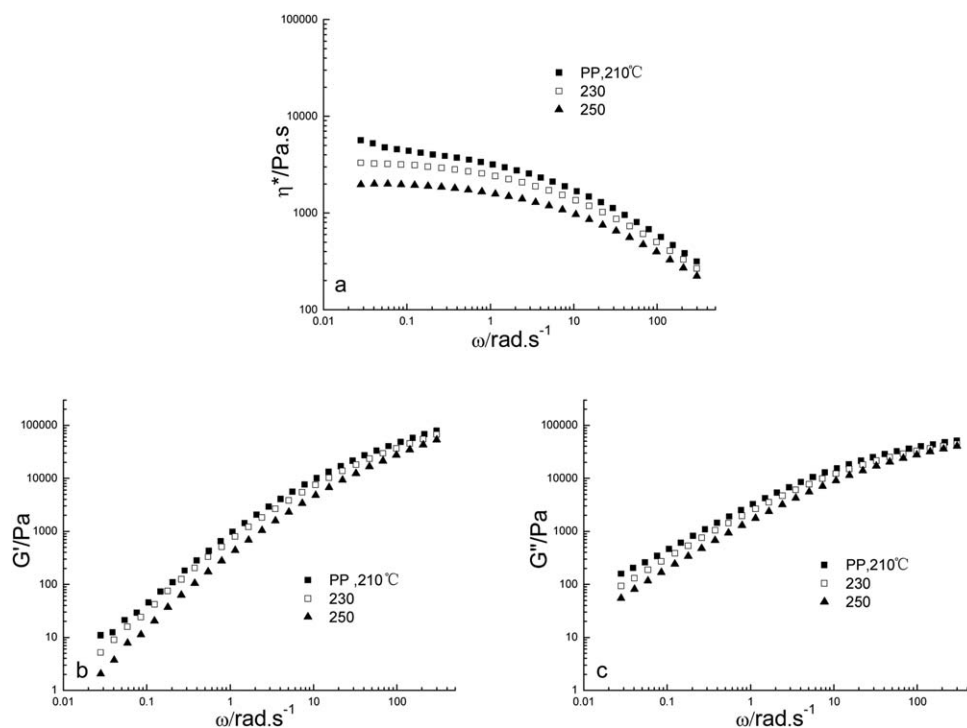


**Figure 2.** (a) Complex viscosity, (b) storage modulus, and (c) loss modulus versus angular frequency of PP at 210, 230, and 250 °C, respectively.

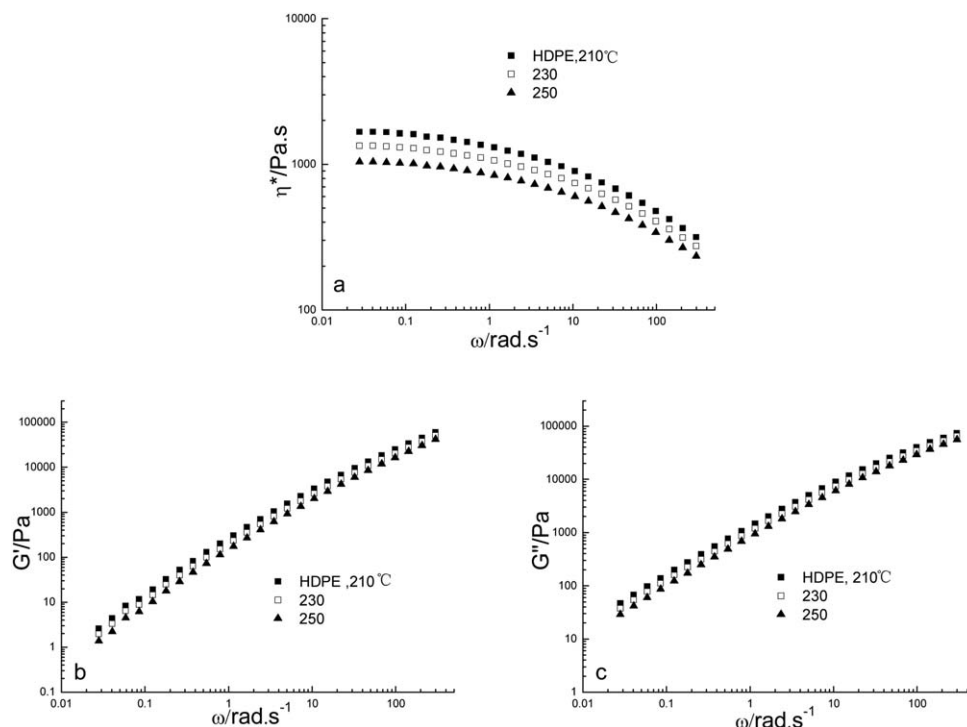
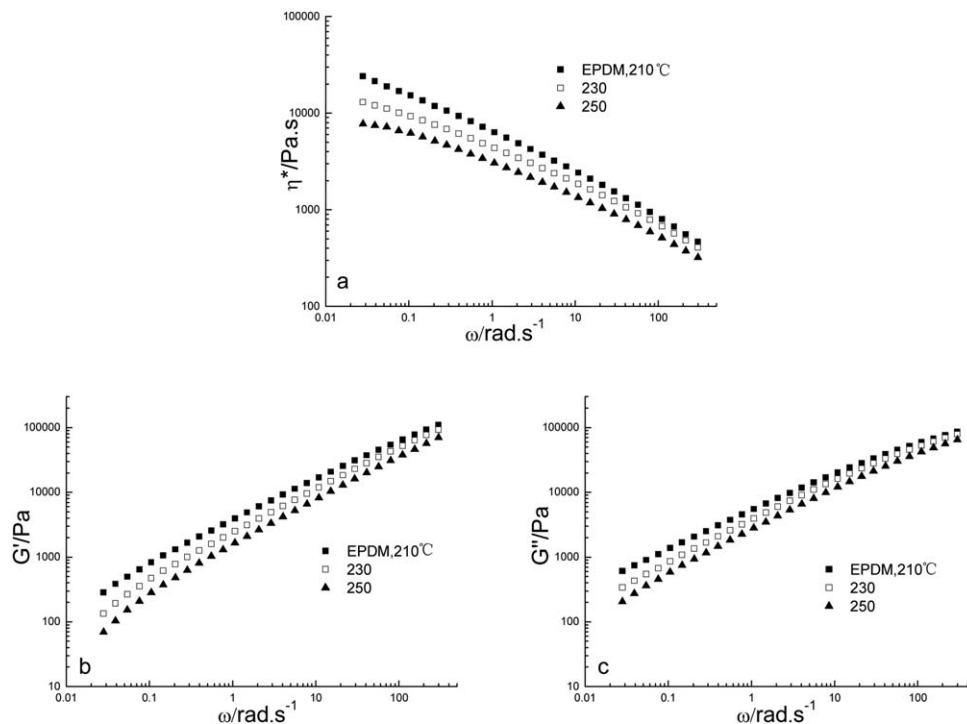


**Figure 3.** (a) Complex viscosity, (b) storage modulus, and (c) loss modulus versus angular frequency of HDPE at 210, 230, and 250 °C, respectively.

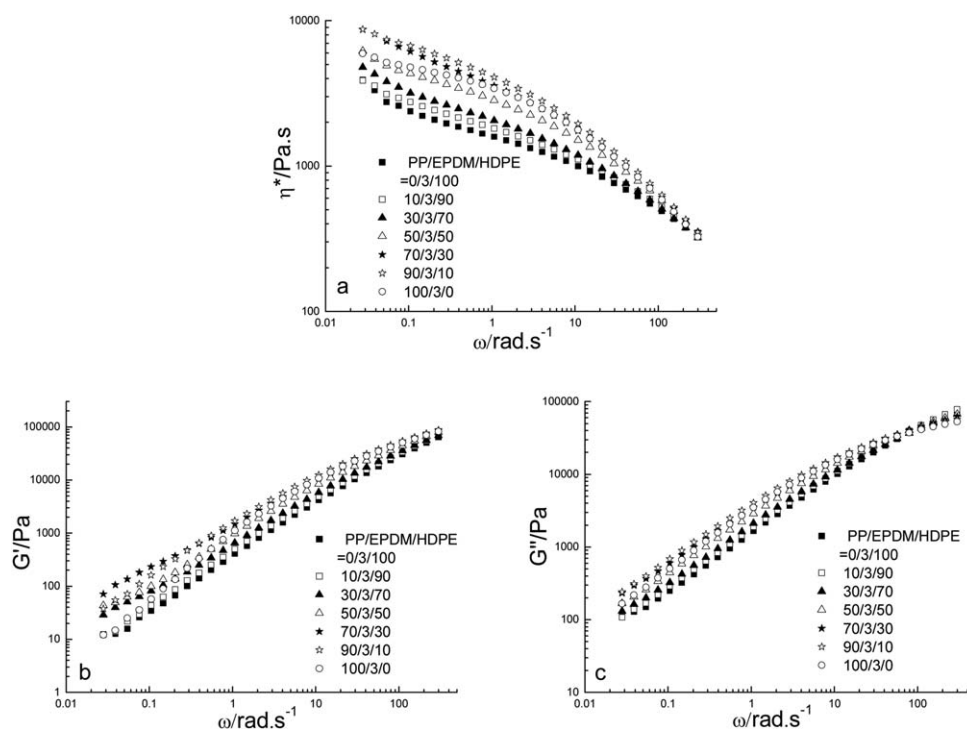
dynamic modulus at low frequency. The first-increase-then-drop trend of the blends means occurrence of phase inversion. At low frequency, the interfacial tension between the blend plays a role.<sup>18</sup>

Figure 6(a–e) show the Cole–Cole diagrams of loss modulus ( $G''$ ) vs.  $G'$  for PP/EPDM/HDPE blends with fixed EPDM = 3 wt % at

210, 230, and 250 °C respectively. In general temperature independence of  $G''$  vs.  $G'$  plots can hold for multicomponent/multi-phase polymer systems.<sup>19</sup> This is the case for most PP/EPDM/HDPE blends as shown in Figure 6. However, the 90/3/10 PP/EPDM/HDPE blend obviously shows temperature dependence at



**Figure 4.** (a) Complex viscosity, (b) storage modulus, and (c) loss modulus versus angular frequency of EPDM at 210, 230, and 250 °C, respectively.



**Figure 5.** (a) Complex viscosity, (b) storage modulus, and (c) loss modulus versus angular frequency of PP/EPDM/HDPE blends at 210 °C.

low and medium frequencies. As temperature increases the storage modulus ( $G'$ ) at fixed loss modulus ( $G''$ ) decreases, as shown by the arrow in Figure 6(e). For the 50/3/50 PP/EPDM/HDPE blend which has co-continuous morphology, no obvious temperature dependence can be observed. This phenomenon is similar to the polylactide/poly( $\epsilon$ -caprolactone) blend in Wu's work.<sup>17</sup> Thus, time-temperature superposition (TTS) principle may be invalid for the 90/3/10 PP/EPDM/HDPE blend.

#### Model Fitting

Some emulsion models such as Palierne's model have been proved successfully to predict the viscoelastic behavior of poly-

mer blends.<sup>10,11,16,17</sup> The dynamic rheology and interfacial tension is related through Palierne's model, the interfacial tension can be obtained if the size of the dispersed phase and the dynamic rheological data of the components are known. The simplified Palierne's model<sup>5,6</sup> is expressed as:

$$G^*(\omega) = G_m^*(\omega) \left[ \frac{1 + 3 \sum_i \phi_i H_i(\omega)}{1 - 2 \sum_i \phi_i H_i(\omega)} \right] \quad (1)$$

where

$$H(\omega) = \frac{4(\alpha/R)[2G_m^*(\omega) + 5G_d^*(\omega)] + [G_d^*(\omega) - G_m^*(\omega)][16G_m^*(\omega) + 19G_d^*(\omega)]}{40(\alpha/R)[G_m^*(\omega) + G_d^*(\omega)] + [2G_d^*(\omega) + 3G_m^*(\omega)][16G_m^*(\omega) + 19G_d^*(\omega)]} \quad (2)$$

$\alpha$  is interfacial tension,  $\phi$  is the volume fraction of the dispersed phase,  $R$  is the dispersed particle radius,  $G_d^*$  and  $G_m^*$  is the complex modulus of the dispersed phase and matrix, respectively. The  $G''$  vs.  $G'$  plots of the blends fitted by Palierne's model are shown using solid line in Figure 6(a-e). The weight ratio of EPDM to (PP + HDPE) is 3 wt %, for the sake of simplification, the PP is considered to be the dispersed phase and HDPE + EPDM to be the matrix when the former is minor phase and the latter major phase. As shown in Figure 6(a), only the 10/3/90 blend is fitted well by Palierne's model. Experimental data at only one temperature was shown as example. The fitted  $\alpha/R$  is 811, 83, and 61 mPa for the 10/3/90 blend at 210, 230, and 250 °C, respectively. This means the interfacial tension decreases as temperature increases. The ratio of  $\alpha/R$  has dimen-

sion of stress and can be considered as the characteristic stress of interface.<sup>15</sup>

Figure 6 shows Palierne's model underestimate all the  $G''$  vs.  $G'$  data except the 10/3/90 blend. Noting the dynamic modulus at low frequency of most of the blends is higher than that of the 0/3/100 and 100/3/0 blend as shown in Figure 5 and only EPDM has higher dynamic modulus than that of most of the blends by comparing Figures 4 and 5, thus EPDM is the key to balance the low dynamic modulus of HDPE and PP. The importance of EPDM in the ternary blends should be paid attention. The aforementioned approach, i.e., taking PP as a phase and taking HDPE + EPDM as another phase is questionable and should be reconsidered. Since EPDM is a physical compatibilizer and lies in the interface between PP and HDPE,

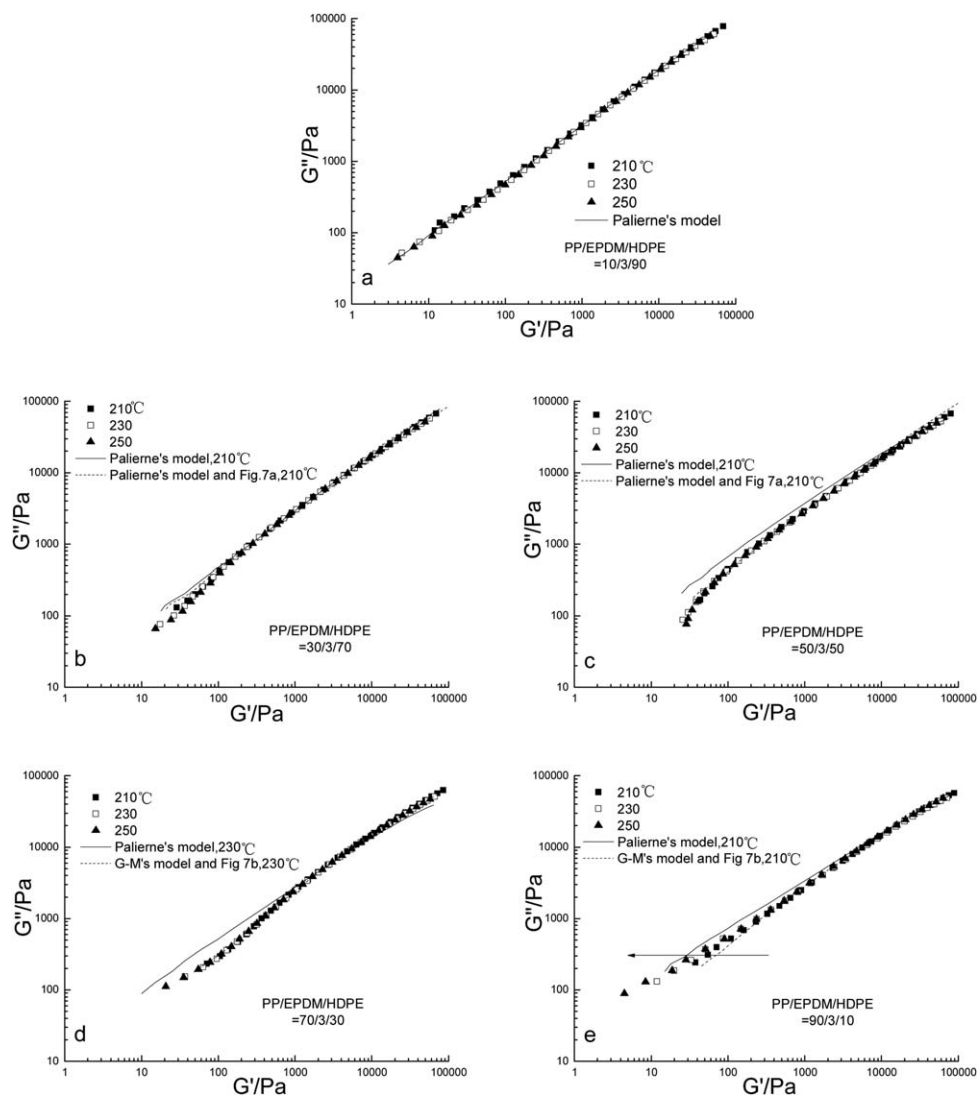


**Figure 6.** Cole–Cole diagram of  $G''$  vs.  $G'$  for PP/EPDM/HDPE blends at 210, 230, and 250 °C.

and the viscosity and dynamic modulus of EPDM are much higher than those of PP and HDPE, it is reasonable to renew the aforementioned approach. A physical scheme is suggested as follows: in the blends, the dispersed droplets are enclosed by EPDM. When PP is the minor phase, PP enclosed by EPDM can be regarded as a phase and HDPE another phase. Similarly, when HDPE is the minor phase, HDPE enclosed by EPDM can be taken as a phase and PP another phase. The scheme is shown in Figure 7. In Figure 7(a), PP is enclosed by EPDM, according to our suggestion EPDM including PP as a whole is considered as the dispersed phase, which is equivalent to an “expanded” EPDM phase, its volume fraction is the sum of that of real EPDM and PP. For the sake of clarification only one dispersed droplet is showed. Similarly in Figure 7(b), the dispersed phase is also the “expanded” EPDM, its real component is HDPE-in-EPDM. In such a manner, the ternary blend is simplified to be a binary blend. For this ‘new’ binary blend Palierne’s model may give a new prediction.

According to Figure 7, Palierne’s model was applied to fit the  $G''$  vs.  $G'$  data, the results are shown by dash line in Figure 6(b,c). For the sake of clarification, only data at 210 °C is shown. Comparing with the solid line in Figure 6(b,c), the fitting curves at low and medium for 30/3/70 and 50/3/50 blends are better, especially for the 50/3/50 blend. It is interesting that using the physical scheme shown in Figure 7 the  $G''$  vs.  $G'$  data of blends with semi-co-continuous and co-continuous morphology can be fitted by Palierne’s model. The predicted interfacial tension divided by droplet diameter  $\alpha/R$  is 0 for 30/3/70 and 50/3/50 blend, respectively. This means the EPDM phase is miscible with HDPE phase. The fitting curves at low frequency are very close to the experimental data. This means the physical scheme in Figure 7 is meaningful. For the 30/3/70 and 50/3/50 blend at 230 and 250 °C, Palierne’s model fails to fit the  $G''$  vs.  $G'$  data, and no obvious improvement happens by combining Palierne’s model with our model shown in Figure 7(a). With the increase of temperature coalescence of droplets may happen,

a dynamic equilibrium may renew during the evolution of the morphology. In fact, Palierne's model is only applicable to droplet/matrix morphology. For the PP-rich blends, the prediction of Palierne's model shows considerable deviations, as shown by the solid line in Figure 6(d,e). As for the failure prediction for PP-rich blends, it may be attributed to the asymmetric viscoelasticity between PP and HDPE. In the work of Chen and Wu,<sup>20</sup> the highly asymmetric in their viscoelasticity of the Poly(trimethylene terephthalate)/poly(butylene succinate) (PTT/PBS) blends affects the description of Palierne's emulsion model. At the same temperature PP has higher elasticity and viscosity than HDPE. For PP-rich blends, PP phase dominates the relaxation of viscoelastic phase interface. For our model shown in Figure 7(b), the dispersed phase is considered to be 'expanded' EPDM, which also has much higher elasticity and viscosity than PP. In this case Palierne's model cannot fit the  $G''$  vs.  $G'$  data well. Now another model, G-M's model should be mentioned. G-M's model is usually applied to fit the dynamic modulus of polymer blend in consideration of the contribution of interface. The following equation is the G-Ms model<sup>11</sup>:

$$G^*(\omega) = \phi G_d^*(\omega) + (1-\phi)G_m^*(\omega) + G_{int}^*(\omega) \quad (3)$$

$$G'(\omega) = \phi G'_d(\omega) + (1-\phi)G'_m(\omega) + \frac{\eta}{\tau_1} \left(1 - \frac{\tau_2}{\tau_1}\right) \frac{\omega^2 \tau_1^2}{1 + \omega^2 \tau_1^2} \quad (4)$$

$$G''(\omega) = \phi G''_d(\omega) + (1-\phi)G''_m(\omega) + \frac{\eta}{\tau_1} \left(1 - \frac{\tau_2}{\tau_1}\right) \frac{\omega \tau_1}{1 + \omega^2 \tau_1^2} \quad (5)$$

with

$$\eta = \eta_m \left[ 1 + \left( \frac{5K+2}{2K+2} \right) \phi + \left( \frac{5(5K+2)^2}{8(K+1)^2} \right) \phi^2 \right] \quad (6)$$

$$\tau = \left( \frac{\eta_m R}{\alpha} \right) \frac{(19K+16)(2K+3)}{40(K+1)} \left( 1 + \phi \frac{5(19K+16)}{4(K+1)(2K+3)} \right) \quad (7)$$

$$\tau = \left( \frac{\eta_m R}{\alpha} \right) \frac{(19K+16)(2K+3)}{40(K+1)} \left( 1 + \phi \frac{3(19K+16)}{4(K+1)(2K+3)} \right) \quad (8)$$

where  $\eta$ ,  $\eta_m$ ,  $\eta_d$  are the Newtonian viscosities of the blend, matrix and dispersed phase, respectively.  $K = \eta_d/\eta_m$  is the viscosity ratio.  $\alpha$  is the interfacial tension between the components of the blend.  $\phi$  is the volume fraction of dispersed phase,  $G^*(\omega)$ ,  $G'_d(\omega)$ ,  $G'_m(\omega)$ , and  $G_{int}^*(\omega)$  is complex modulus of the blend, the dispersed phase, the matrix and interface, respectively. Using the physical scheme shown in Figure 7(b), the fitting results by G-M's model with assuming  $G_{int}^*(\omega)$  zero are also shown in Figure 6(d,e). Assuming  $G_{int}^*(\omega)$  to be zero means the blend is miscible. For the PP-rich blends, such as 70/3/30 and 90/3/10 blends, G-M's model combined with our model predicts the  $G''$  vs.  $G'$  data well. This is the case for the three temperatures. It means PP and HDPE phase is miscible in PP-rich blends. For HDPE-rich blends, combination of the physical scheme shown in Figure 7(a) and G-M's model with assuming  $G_{int}^*(\omega)$  zero overestimates the  $G''$  vs.  $G'$  data, which are not shown in this work. Obviously larger deviations may occur if  $G_{int}^*(\omega)$  is not neglected in G-M's model. For the G-M's model three contributions, i.e., two phases and an interface control blend dynamic moduli.<sup>14</sup> G-M's model usually fails to show an adequate fit and predict admissible values for interfacial tension for polymer blends with excessive large difference between the zero-shear viscosities. For the HDPE-rich blends, the viscosity ratio at 210 °C of

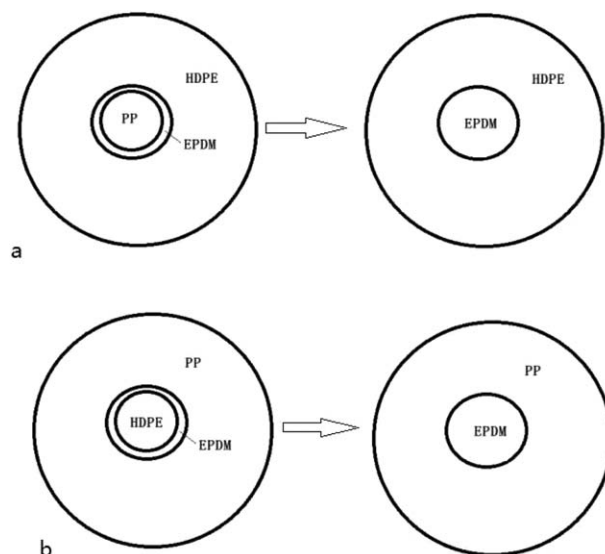


**Figure 7.** Physical scheme of the PP/EPDM/HDPE ternary blends, (a) HDPE-rich blend, (b) PP-rich blend.

EPDM to HDPE at 0.028 rad s<sup>-1</sup> is 14.4, much higher than that of EPDM to PP, i.e., 4.3 for the HDPE-rich blends.

## CONCLUSIONS

Dynamic rheological behaviors of the PP/EPDM/HDPE blends at 210, 230, and 250 °C are investigated by experimental method as well as model fitting. At the same temperature the pure EPDM has higher viscoelasticity than PP, and PP has higher than HDPE. The 30/3/70 blend has semi-co-continuous morphology, the 50/3/50 blend has co-continuous morphology, and the 70/3/30 blend has droplet/matrix morphology.

At three temperatures 210, 230, and 250 °C the simplified Palierne's model cannot fit well the Cole-Cole ( $G''$  vs.  $G'$ ) data for the blends except the 10/3/90 blend. Then a physical scheme based on the structure of the PP/EPDM/HDPE blends is proposed that the dispersed droplets (the minor phase) is enclosed by EPDM. Thus the ternary blend is composed of two phase: the dispersed 'expanded' EPDM phase and the matrix. With this physical scheme Palierne's model can fit the  $G''$  vs.  $G'$  data for the 30/3/70 and 50/3/50 blends at 210 °C. Also with the physical scheme G-M's model with interfacial  $G_{int}' = 0$  can fit the dynamic modulus data ( $G'$  and  $G''$ ) for the PP-rich blends at 210, 230, and 250 °C. However the  $G'$  data for the 30/3/70 blend and the 50/3/50 blend at 230 and 250 °C cannot be fit well by either Palierne's model or G-M's model with interfacial  $G' = 0$ . This maybe due to the complex morphology of the blend. In consideration of most of dynamic modulus data of the blends can be fitted by Palierne's model as well as G-M's model, the proposed physical scheme may be reasonable. Further development of the physical scheme in fitting the dynamic data will be done in future.

## ACKNOWLEDGMENTS

This work is supported by Science and Technology Department of Jiangsu Province science and technology projects of China (No. BY2015027-25).

## REFERENCES

1. Chopra, D.; Kontopoulou, M.; Vlassopoulos, D.; Hatzikiriakos, S. G. *Rheol. Acta* **2002**, *41*, 10.
2. Xing, P. X.; Bousmina, M.; Rodrigue, D. *Macromolecules* **2000**, *33*, 8020.
3. Utracki, L. A. *Two Phase Polymer Systems*; Hanser Publisher, New York, **1991**.
4. Jafari, S. H.; Hesabi, M. N.; Khonakdar, H. A.; Asl-Rahimi, M. J. *Polym. Res.* **2011**, *18*, 821.
5. Palierne, J. F. *Rheol. Acta* **1990**, *29*, 204.
6. Asthana, H.; Jayaraman, K. *Macromolecules* **1999**, *32*, 3412.
7. Bousmina, M. *Rheol. Acta* **1999**, *38*, 73.
8. Lacroix, C.; Bousmina, M. P.; Carreau, J.; Favis, B. D. *Polymer* **1996**, *37*, 2939.
9. Lee, H. M.; Park, O. O. J. *Rheology* **1994**, *38*, 1405.
10. Kim, H. J.; Seo, Y. *Langmuir* **2003**, *19*, 2696.
11. Gramespacher, H.; Meissner, J. J. *Rheology* **1992**, *36*, 1127.
12. Liao, H. Y.; Qi, L. Y.; Tao, G. L.; Liu, C. L. *Polym. Bull.* **2015**, *72*, 1197.
13. Tabatabaei, S. H.; Carreau, P. J.; Ajji, A. *Chem. Eng. Sci.* **2009**, *64*, 4719.
14. Choi, S. J.; Schowalter, W. R. *Phys. Fluids* **1975**, *18*, 420.
15. Kwon, M. K.; Cho, K. S. *Kor. Aust. Rheol. J.* **2016**, *28*, 23.
16. Shi, D. A.; Ke, Z.; Yang, J. H.; Gao, Y.; Wu, J.; Yin, J. H. *Macromolecules* **2002**, *35*, 8005.
17. Wu, D. F.; Zhang, Y. S.; Zhang, M.; Zhou, W. D. *Eur. Polym. J.* **2008**, *44*, 2171.
18. Yu, W.; Zhou, W.; Zhou, C. X. *Polymer* **2010**, *51*, 2091.
19. Han, C. D. *Multiphase flow in Polymer Processing*; Academic Press, New York, **1981**.
20. Chen, J. X.; Wu, D. F. *Mater. Chem. Phys.* **2014**, *148*, 554.
21. Vinckier, I.; Moldenaers, P.; Mewis, J. J. *Rheology* **1996**, *40*, 613.